# Northumbria Research Link

# A system model of three-body interactions in complex networks: Consensus and conservation

Yilun Shang*

Department of Computer and Information Sciences,
Northumbria University, Newcastle upon Tyne NE1 8ST, UK

## Abstract

Networked complex systems in a wide range of physics, biology and social sciences involve synergy among multiple agents beyond pairwise interactions. Higher-order mathematical structures such as hypergraphs have been increasingly popular in modelling and analysis of complex dynamical behaviors. Here, we study a simple three-body consensus model, which favorably incorporates higher-order network interactions, higher-order dimensional states, group reinforcement effect as well as social homophily principle. The model features asymmetric roles of acting agents using modulating functions. We analytically establish sufficient conditions for nonlinear consensus and conservation of states for agents with both discrete-time and continuous-time dynamics. We show that higher-order interactions encoded in three-body edges give rise to consensus and conservation for systems with gravity-like and Heaviside-like modulating functions. Furthermore, we illustrate our theoretical results with numerical simulations and examine the system convergence time through a network depreciation process.

**Keywords:** higher-order interaction, higher-dimension, complex network, consensus, conservation law, nonlinear dynamics

## 1    Introduction

Complex networks have the ability to model many natural and man-made systems composed of interacting units [1, 2]. The overall system behavior

---

*Correspondence:  yilun.shang@northumbria.ac.uk

is governed by its nodes, whose states are influenced by neighboring nodes through connecting edges in the network. Understanding the interaction between network components and how it shapes the collective dynamics of the entire complex system is therefore of transdisciplinary interest.

In the conventional network representation of complex systems, a dominating hypothesis is that basic interacting units in networks are captured exclusively by pairwise interactions. This assumption is often not verified in diverse real-world systems such as neuroscience [3, 4, 5], ecological systems [6, 7] and scientific collaboration [8, 9], where essential interplay takes place at a collective level involving group or multibody interactions [10, 11, 12]. Examples include the presence of higher-order neuronal connection patterns in human brain networks to support nervous activities and cognitive processes [13]; social changes require complex contagions with multiple exposures and group social interactions [14]; and species coexistence and biodiversity can be promoted in an ecosystem if three or more species are factored in the species competition relationship [15]. Distinct from pairwise interactions, higher-order interactions account for the group effect as a whole, which cannot be regarded as a combination effect of dyadic connections.

To account for higher-order organization of complex systems and its structural and dynamical implications, the building blocks of network structure have been extended from pairs of nodes to small subgraphs and motifs [16, 17]. Higher-order network architectures are often described by hypergraphs, Petri nets, and simplicial complexes. A simplicial complex can be formed by binding simplexes along their faces of any dimension, where a $k$-simplex is a filled clique of $k + 1$ nodes for $k \geq 1$ [18]. With their origin in algebraic topology and the geometric interpretation, simplicial complexes have been found very useful in the analysis of high-dimensional topological data [19, 20, 21]. Hypergraphs [22, 23] allow interaction between nodes through hyperedges consisting of any number of nodes such as pairs (conventional two-body edges), triples (three-body edges), quadruples (four-body edges) etc. Petri nets [24] are an important kind of directed hypergraphs, which underpin the finite-state machine theory in theoretical computer science [25]. Different from the simplicial complex approach, the hypergraph approach does not require the existence of all lower-order interactions. A range of dynamical processes such as social contagion [14, 26], oscillator synchronization [27, 28], random walks [29, 30], opinion dynamics [31, 32] and naming games [33] have been studied on these higher-order system models in the last few years.

On the other hand, consensus over networks has become a major research topic with applications across a wide spectrum of fields including physics,

2

engineering, biology and social science. In a consensus problem [34], a group of agents reach a common state through local information exchange through the underlying communication network. Consensus problems have been investigated extensively in both discrete-time and continuous-time models [35, 36, 37, 38, 39, 40]. In tandem with the recent flurry of research enthusiasm in multibody interactions, consensus problems have been generalized to accommodate these higher-order models. In [41], a continuous-time consensus framework is developed over simplicial complex structures by using the gradient flow of an energy functional. A continuous-time multibody consensus model is proposed in [42, 43] incorporating group reinforcement on hypergraphs. It is unraveled that linear consensus protocols are not able to model genuine higher-order interactions. Building on the siphon theory of Petri net, the author [24] studies a continuous-time opinion dynamic model with bounded confidence and observer effect. It is shown that consensus state can be reached asymptotically via higher-order neighbor-dependence synergy.

Motivated by this line of research, we here propose a three-body consensus dynamical model over hypergraphs featuring asymmetric roles in triples with both primary and secondary agents. The update rule of an agent $i$ that forms a hyperedge with a primary agent $j$ and a secondary agent $k$ depends on the diffusive interaction with $j$ and the modulating action of $k$ on both $i$ and $j$. By specifying different roles in a triple, we put together a nonlinear dynamical system that incorporates reinforcing group effect and homophily. Our framework for consensus has some differences compared with the existing works [24, 41, 42, 43]. First, we propose both discrete-time and continuous-time system models whereas only continuous-time models are considered previously. Second, unlike the above works dealing with only scalars, we consider general vector states. Third, we develop analytical frameworks and provide rigorous proof in addition to numerical simulations. In the case of gravity-like modulating functions with infinite supports, both discrete-time and continuous-time models are shown to achieve consensus when the interaction hypergraph is connected and the modulating functions satisfy some mild conditions. In the case of modulating functions with finite supports, in order to ensure consensus in both models, we propose sufficient conditions on the initial state configuration in terms of some energy functions. Fourth, the ultimate consensus state is shown to be the average of initial states of agents. Hence, average consensus is achieved. As the number of agents in the system is fixed, our model is capable of conserving total states over the system at all times.

The remainder of the paper is organized as follows. Section 2 provides the

nonlinear three-body dynamical models. Section 3 and Section 4 are devoted to the analysis of discrete-time and continuous-time systems, respectively. Numerical studies are presented in Section 5. Conclusions in Section 6 end the paper.

# 2 Consensus dynamics with three-body interactions: asymmetric roles

The object of this study is $n$ coupled dynamical agents, whose interconnection network structure is encoded in a hypergraph $\mathcal{G} = (\mathcal{V}, \mathcal{E}, \mathcal{A})$ with the node set $\mathcal{V} = \{1, 2, \cdots, n\}$ and the edge set $\mathcal{E} = \{\{i, j, k\} | i, j, k \in \mathcal{V}\}$. Here, $\mathcal{E}$ consists of unordered triples or triangles (three-body edges), and the associated adjacency tensor is given by $\mathcal{A} = (a_{ijk}) \in \mathbb{R}^{n \times n \times n}$ with $a_{ijk} = 1$ if $\{i, j, k\} \in \mathcal{E}$ and $a_{ijk} = 0$ otherwise. We assume $a_{ijk} = 0$ if the triple is degenerate, namely $i = j$, $i = k$ or $j = k$. Two nodes $i$ and $j$ are said to be adjacent if they are in the same edge in $\mathcal{E}$. Two nodes $i$ and $j$ are connected if there is a list of nodes starting from $i$ and ending at $j$, every two contiguous nodes of which are adjacent. Accordingly, $\mathcal{G}$ is called connected if each pair of nodes is connected in $\mathcal{G}$. The hypergraph $\mathcal{G}$ is a natural counterpart for a undirected graph structure characterizing interactions over two-body edges [10]. From a graph theory perspective, $\mathcal{G}$ is a 3-uniform hypergraph. In other words, it only characterizes three-body edges and no edges (interactions) of other orders are considered. For simplicity, we will just use the word 'edge' to represent edge of any order if the meaning is clear from the context.

The equations of evolution governing the dynamics of agents in $\mathcal{G}$ are given by

$$x_i(t + 1) = x_i(t) + h u_i(t), \quad i \in \mathcal{V}, \ t = 0, 1, 2, \cdots \tag{1}$$

for discrete-time system, and

$$\dot{x}_i(t) = u_i(t), \quad i \in \mathcal{V}, \ t \geq 0 \tag{2}$$

for continuous-time system, where $h > 0$ is a regulation constant, $x_i(t) \in \mathbb{R}^m$ is the state vector of agent $i$ and $u_i(t) \in \mathbb{R}^m$ is the interaction function describing the coupling strength as well as influence of other agents on agent $i$. The state space of agents is assumed to be $m$-dimensional while previous studies [24, 41, 42, 43] focus on the low-dimension case of $m = 1$. We propose

4

an interaction function written as

$$u_i(t) = \sum_{j,k=1}^{n} a_{ijk} g(\|x_i(t) - x_j(t)\|) g_k^I(\|x_i(t) - x_k(t)\|) g_k^I(\|x_j(t) - x_k(t)\|)$$

$$\cdot g_k^{II}\left(\left\|\frac{x_i(t) + x_j(t)}{2} - x_k(t)\right\|\right)(x_j(t) - x_i(t)), \tag{3}$$

where $\|\cdot\|$ represents the Euclidean norm, each triple of affected node $i$, primary acting node $j$ and secondary acting node $k$ is modulated by functions $g$, $g_k^I$ and $g_k^{II}$. We consider two commonly used classes of functions for these modulating functions $g$, $g_k^I$ and $g_k^{II}$. The first class is gravity-like functions. Namely,

$$\mathcal{F}_1 = \{f : [0, \infty) \rightarrow (0, \infty) | f(y_1) \geq f(y_2) \text{ if } y_1 \leq y_2\}. \tag{4}$$

These functions are non-increasing and have infinite supports. The second class is made up of Heaviside-like functions:

$$\mathcal{F}_2(\sigma, \phi) = \{f : [0, \infty) \rightarrow [0, \infty) | f(y) \equiv 0 \text{ for } y \geq \sigma > 0; f(y) \geq \phi > 0$$
$$\text{for } y < \sigma; \ f(y_1) \geq f(y_2) \text{ if } y_1 \leq y_2\}. \tag{5}$$

The functions in $\mathcal{F}_2(\sigma, \phi)$ are also monotonic and have a positive lower bound $\phi$ over the support set $[0, \sigma)$.
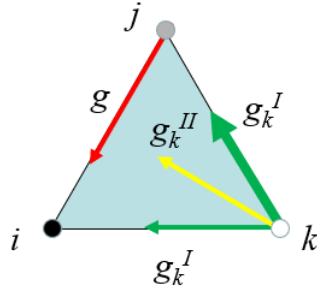


Figure 1: Schematic of a three-body edge $\{i, j, k\}$ with $i$ being the affected node, $j$ the primary acting node and $k$ the secondary acting node. As the states of $j$ and $k$ are closer (as the color indicated), the modulation along $\{j, k\}$ is stronger compared to that along $\{i, k\}$.

The three nodes in an edge $\{i, j, k\}$ with $a_{ijk} = 1$ have asymmetric roles in (3). For the affected node $i$, we view $j$ as the primary acting node and $k$ the secondary acting node; c.f. Fig. 1. The modulating function

$g(\|x_i(t) - x_j(t)\|)$ models the homophily principle in social networks [44, 45] or the visual distance in Euclidean space. For the latter, note that the Cucker-Smale flocking model [46, 47] offers an example of $g \in \mathcal{F}_1$ and Vicsek model [48] is an example of $g \in \mathcal{F}_2$. This modulating function together with a linear diffusive coupling, i.e., the last term in (3), has been extensively investigated in many dynamical systems over graphs such as consensus and synchronization problems [2, 34]. In our hypergraph setting, the action of the secondary node $k$ is captured by two possible types of modulating functions $g_k^I$ and $g_k^{II}$. Both of them reflect a reinforcing group effect among the three nodes in an edge, where closer nodes states give rise to a higher modulation weight. The function type $g_k^I$ gives a sense of 'separation of variables' while the type $g_k^{II}$ treats the two neighbors $i$ and $j$ as a whole. Clearly, if any of these functions are in the class $\mathcal{F}_1$, we can freely choose them as a constant function to adjust modulation mechanism in (3).

The introduction of nonlinear modulating functions is inspired by the works [42, 43]. In addition to the differences discussed in Section 1, the asymmetric roles introduced in the current model allows the system to preserve the total states (see Definition 2 below), which are not achievable in [42, 43]. There are some examples in which our notion of asymmetric roles of the primary and secondary acting nodes is of interest. In practical scenarios such as distributed bird flocks, driving in a traffic, and social and animal hierarchies, it is prevalent to have systems that are organized into a hierarchical influence or leadership structure [49, 50], where nodes at a lower level look up to nodes at higher levels (see e.g. [51, Fig. 1]). In our setting, the primary node $j$ influences $i$ through $g$ and the secondary node $k$ influences $i$ and $j$ through $g_k^I$ and $g_k^{II}$. The effective role of a secondary node $k$ as a reference providing adjustment or recommendation has been highlighted in some friend finder algorithms in social network analysis [52]. A similar distance-modulated mechanism is also adopted in the study of higher-order interaction for species coexistence [53], where the biotic interaction between a focal tree ($i$) and a neighboring tree ($j$) is modulated by an intermediary tree ($k$). Tree survival and growth is shown to be better predicted with this approach.

We are interested in two important properties of the system regarding the equilibrium and transient evolution, namely, whether the ultimate states of the coupling agents will reach a common state vector and how will the total or average state over the entire system evolve. Formally, we have the following definitions. Let $x(t) = (x_1(t)^{\mathsf{T}}, x_2(t)^{\mathsf{T}}, \cdots, x_n(t)^{\mathsf{T}})^{\mathsf{T}} \in \mathbb{R}^{nm}$, where $\mathsf{T}$ represents the transpose operator.

**Definition 1. (Consensus)** Consensus for the system is said to be achieved

if for any initial configuration of $x(0) \in \mathbb{R}^{nm}$, $\lim_{t \to \infty} \|x_i(t) - x_j(t)\| = 0$ holds true for all $i, j \in \mathcal{V}$.

**Definition 2. (Conservation)** Conservation for the system is said to be achieved if for any initial configuration of $x(0) \in \mathbb{R}^{nm}$, $\sum_{i=1}^{n} x_i(t) = \sum_{i=1}^{n} x_i(0)$ for all $t \geq 0$.

Clearly, if both consensus and conservation can be reached, we obtain the average consensus $\lim_{t \to \infty} x_i(t) = \frac{1}{n} \sum_{i=1}^{n} x_i(0)$.

# 3 Consensus and conservation of discrete-time dynamics

We will analyze the discrete-time system (1) in this section and defer the continuous-time system (2) to Section 4. To set the scene for later development, let $\mathcal{T}_{ij}$ be the set of nodes in $\mathcal{G}$ such that there exists a three-body edge with the other two nodes being $i$ and $j$. Obviously, the cardinality $|\mathcal{T}_{ij}|$ counts the number of triangles in $\mathcal{G}$ sharing a common edge $\{i, j\}$. Given $i, j \in \mathcal{V}$, define

$$b_{ij}(t) = \sum_{k=1}^{n} a_{ijk} g(\|x_i(t) - x_j(t)\|) g_k^I(\|x_i(t) - x_k(t)\|) g_k^I(\|x_j(t) - x_k(t)\|)$$

$$\cdot g_k^{II}\left(\left\|\frac{x_i(t) + x_j(t)}{2} - x_k(t)\right\|\right). \tag{6}$$

In the following, we sometimes choose to suppress the time $t$ and write notations like $b_{ij}$ and $x_i$ for ease of reading. Feeding (6) into (3), we have a time-dependent linear feedback

$$u_i(t) = \sum_{j=1}^{n} b_{ij}(t)(x_j(t) - x_i(t)). \tag{7}$$

We define the diagonal degree matrix for the system as $\mathcal{D} = \text{diag}(d_{11}, d_{22}, \cdots, d_{nn}) \in \mathbb{R}^{n \times n}$, where $d_{ii} = \sum_{j=1}^{n} b_{ij}$. The corresponding Laplacian matrix is given by $\mathcal{L} = \mathcal{D} - \mathcal{B}$, where $\mathcal{B} = (b_{ij}) \in \mathbb{R}^{n \times n}$. It is worth noting that these matrices are not functions of the hypergraph topology as opposed to classic consensus theory [34, 35]. They encode both the higher-order network architecture and nonlinear (higher-dimensional) agent dynamics.

## 3.1 Gravity-like modulating functions

We first consider the conservation and consensus of the discrete-time system (1) when the modulating functions are all gravity-like.

7

For $i \in \mathcal{V}$, let $\Delta_i = \frac{1}{2} \sum_{j=1}^n |\mathcal{T}_{ij}|$ count the number of triangles, i.e. three-body edges, that $i$ is in. Denote by $\Delta_{\max} = \max_{i \in \mathcal{V}} \Delta_i$. In general, the number of $d$-body edges connected to a node is also known as generalised degree [54].

**Theorem 1.** *Assume $g, g_k^I, g_k^{II} \in \mathcal{F}_1$ for all $k \in \mathcal{V}$ and $\mathcal{G}$ is connected. If $h \in \left(0, (2\Delta_{\max} g(0) \max_{k \in \mathcal{V}}\{g_k^I(0)^2 g_k^{II}(0)\})^{-1}\right)$, then the discrete-time system (1) with (3) achieves consensus and conservation.*

**Proof.** Recall that $x(t) = (x_1(t)^\mathsf{T}, x_2(t)^\mathsf{T}, \cdots, x_n(t)^\mathsf{T})^\mathsf{T}$ for $t \geq 0$. By (1) and (3) we obtain a compact form

$$x(t+1) = x(t) - h(\mathcal{L} \otimes I_m)x(t), \tag{8}$$

where $I_m \in \mathbb{R}^{m \times m}$ is the identity matrix and $\otimes$ is the Kronecker product. Let $\mathcal{M} = \text{span}\{1_n \otimes z | z \in \mathbb{R}^m\} \in \mathbb{R}^{nm}$ be the synchronization manifold and $P_\mathcal{M}$ be the projection operator over $\mathcal{M}$, where $1_n \in \mathbb{R}^n$ represents the all-one vector. It is not difficult to check that $P_\mathcal{M} x = 1_n \otimes \frac{1}{n} \sum_{i=1}^n x_i$. Applying $P_\mathcal{M}$ on both sides of (8) yields

$$P_\mathcal{M} x(t+1) = P_\mathcal{M} x(t) - h(\mathcal{L} \otimes I_m)P_\mathcal{M} x(t), \tag{9}$$

where we have used $\mathcal{L}^\mathsf{T} = \mathcal{L}$ and $\mathcal{L}1_n = 0_n$ for any time $t$. Here, $0_n \in \mathbb{R}^n$ is the all-zero vector. Let $\xi(t) = x(t) - P_\mathcal{M} x(t)$ be the difference. We aim to show that $\xi$ is vanishing as $t$ tends to infinity.

Combining (8) and (9), we obtain

$$\xi(t+1) = \xi(t) - h(\mathcal{L} \otimes I_m)\xi(t). \tag{10}$$

Define $\theta(t) = \xi(t)^\mathsf{T} \xi(t)$ and we obtain by (10)

$$\begin{aligned}
\theta(t+1) - \theta(t) &= \xi(t)^\mathsf{T}((I_n - h\mathcal{L}) \otimes I_m)^2 \xi(t) - \xi(t)^\mathsf{T} \xi(t) \\
&= -\xi(t)^\mathsf{T}(\Theta(t) \otimes I_m)\xi(t),
\end{aligned} \tag{11}$$

where $\Theta(t) = 2h\mathcal{L} - h^2\mathcal{L}^2$. Denote the eigenvalues of $\mathcal{L}$ by $\lambda_1(\mathcal{L}) \leq \lambda_2(\mathcal{L}) \leq \cdots \leq \lambda_n(\mathcal{L})$. Note that they are time-dependent. In view of (6) and the assumption $g, g_k^I, g_k^{II} \in \mathcal{F}_1$ for $k \in \mathcal{V}$, we obtain $0 \leq b_{ij}(t) \leq |\mathcal{T}_{ij}|g(0) \max_{k \in \mathcal{V}}\{g_k^I(0)^2 g_k^{II}(0)\}$ for any $t \geq 0$. Using the Gershgorin circle theorem,

$$\lambda_i(\mathcal{L}) \leq 2\max_{i \in \mathcal{V}} \sum_{j=1}^n b_{ij}(t) \leq 4\Delta_{\max} g(0) \max_{k \in \mathcal{V}}\{g_k^I(0)^2 g_k^{II}(0)\} \tag{12}$$

for all $i \in \mathcal{V}$. Since $\lambda_i(\Theta(t)) = h\lambda_i(\mathcal{L})(2 - h\lambda_i(\mathcal{L}))$ and $(2 - h\lambda_i(\mathcal{L})) > 0$ by the condition $h \in \left(0, (2\Delta_{\max} g(0) \max_{k \in \mathcal{V}}\{g_k^I(0)^2 g_k^{II}(0)\})^{-1}\right)$ and (12),

we know that all eigenvalues of $\Theta(t)$ are non-negative and the number of possible zero eigenvalues is equal to the number of zero eigenvalue of $\mathcal{L}$ for any time $t$. Hence, $\Theta(t)$ is positive semidefinite.

Denote by $\hat{\lambda}(\cdot)$ the minimum non-zero eigenvalue of a positive semidefinite matrix and $\mathcal{N}(\cdot)$ its eigenspace corresponding to 0. Since $\mathcal{G}$ is connected, neither $\mathcal{L}$ nor $\Theta(t)$ is a zero matrix. With the observation in the above paragraph, we have $\hat{\lambda}(\Theta(t) \otimes I_m) = \hat{\lambda}(\Theta(t)) > 0$. It follows from (11) and the Rayleigh-Ritz theorem that

$$
\begin{aligned}
\theta(t+1) - \theta(t) \leq & - \hat{\lambda}(\Theta(t)) \cdot \left( \xi(t) - P_{\mathcal{N}(\Theta(t)\otimes I_m)}\xi(t) \right)^{\mathsf{T}} \\
& \cdot \left( \xi(t) - P_{\mathcal{N}(\Theta(t)\otimes I_m)}\xi(t) \right).
\end{aligned}
\tag{13}
$$

As $\mathcal{G}$ is connected, by the assumption $g, g_k^I, g_k^{II} \in \mathcal{F}_1$ for $k \in \mathcal{V}$ we know that $\mathcal{N}(\mathcal{L}) = \mathrm{span}\{z1_n | z \in \mathbb{R}\}$. Therefore, $\mathcal{N}(\mathcal{L} \otimes I_m) = \mathcal{M}$. In light of the definition of $\Theta(t)$, we then have $\mathcal{N}(\Theta(t) \otimes I_m) = \mathcal{M}$. Furthermore, $P_{\mathcal{M}}\xi(t) = P_{\mathcal{M}}x(t) - P_{\mathcal{M}}P_{\mathcal{M}}x(t) = 0_{nm}$. Due to the connectedness of $\mathcal{G}$ and the positiveness of the modulating functions, the right-hand side of (13) is equivalent to

$$
\begin{aligned}
& - \lambda_2(\Theta(t)) \cdot \left( \xi(t) - P_{\mathcal{N}(\Theta(t)\otimes I_m)}\xi(t) \right)^{\mathsf{T}} \left( \xi(t) - P_{\mathcal{N}(\Theta(t)\otimes I_m)}\xi(t) \right) \\
& = - \lambda_2(\Theta(t)) \cdot \xi(t)^{\mathsf{T}}\xi(t) \leq 0
\end{aligned}
\tag{14}
$$

and $\lambda_2(\Theta(t)) > 0$ for any $t \geq 0$. Since $\theta(t) = \|\xi(t)\|^2$, we know $\|\xi(t)\|$ is non-increasing by (13) and (14). Recall that our aim is to show $\xi(t) \to 0_{nm}$ as $t \to \infty$. So we are still one step away.

We will estimate the eigenvalue $\lambda_2(\Theta(t))$ in (14). By assumptions we know $\lambda_2(\mathcal{L}) > 0$ for all $t \geq 0$. Moreover, it has a positive lower bound. In fact, let $\eta = (\eta_1, \eta_2, \cdots, \eta_n)^{\mathsf{T}} \in \mathbb{R}^n$ be the normalized unit eigenvector associated with $\lambda_2(\mathcal{L})$. By direct calculations we have $\max_{i,j \in \mathcal{V}} \|x_i(t) - x_j(t)\| \leq \sqrt{2}\|\xi(t)\|$; see e.g. [55, Lemma 1]. Hence, $\max_{i,j \in \mathcal{V}} \|x_i(t) - x_j(t)\| \leq$

$\sqrt{2}\|\xi(0)\|$. Involving (6) and the assumption $g, g_k^I, g_k^{II} \in \mathcal{F}_1$, we have

$$
\begin{aligned}
\lambda_2(\mathcal{L}) =& \eta^{\mathsf{T}} \mathcal{L} \eta \\
=& \frac{1}{2} \sum_{i,j,k=1}^{n} a_{ijk} g(\|x_i - x_j\|) g_k^I(\|x_i - x_k\|) g_k^I(\|x_j - x_k\|) \\
& \cdot g_k^{II}\left(\left\|\frac{x_i + x_j}{2} - x_k\right\|\right)(\eta_i - \eta_j)^2 \\
\geq& \frac{1}{2} g(\sqrt{2}\|\xi(0)\|) \min_{k \in \mathcal{V}} \left\{ g_k^I(\sqrt{2}\|\xi(0)\|)^2 \right. \\
& \left. \cdot g_k^{II}(\sqrt{2}\|\xi(0)\|) \right\} \sum_{i,j,k=1}^{n} a_{ijk}(\eta_i - \eta_j)^2 \\
=& g(\sqrt{2}\|\xi(0)\|) \min_{k \in \mathcal{V}} \left\{ g_k^I(\sqrt{2}\|\xi(0)\|)^2 g_k^{II}(\sqrt{2}\|\xi(0)\|) \right\} \eta^{\mathsf{T}} \hat{\mathcal{L}} \eta \\
\geq& \, g(\sqrt{2}\|\xi(0)\|) \min_{k \in \mathcal{V}} \left\{ g_k^I(\sqrt{2}\|\xi(0)\|)^2 g_k^{II}(\sqrt{2}\|\xi(0)\|) \right\} \lambda_2(\hat{\mathcal{L}}) := c_1 > 0,
\end{aligned}
$$

$$(15)$$

where $\hat{\mathcal{L}}$ is the Laplacian corresponding to the graph $\hat{\mathcal{G}}$ with $(i, j)$-element of its adjacency matrix being $\sum_{k=1}^{n} a_{ijk}$. Clearly, $\hat{\mathcal{G}}$ is connected and we have relied on Rayleigh-Ritz theorem again in the last inequality of (15).

We have $\lambda_1(\Theta(t)) = 0$ and for $i \geq 2$ we estimate

$$
\begin{aligned}
\lambda_i(\Theta(t)) =& h\lambda_i(\mathcal{L})(2 - h\lambda_i(\mathcal{L})) \\
\geq& hc_1\left(2 - 4h\Delta_{\max} g(0) \max_{k \in \mathcal{V}}\{g_k^I(0)^2 g_k^{II}(0)\}\right) := c_2 > 0
\end{aligned}
$$

$$(16)$$

by using (12), (15) and the assumption of $h$. Combining (13), (14) and (16), we have $\theta(t+1) - \theta(t) \leq -c_2\xi(t)^{\mathsf{T}}\xi(t)$. This indicates $\xi(t) \to 0_{nm}$ as $t \to \infty$. [If this does not hold, there exists some $\varepsilon > 0$ such that $\|\xi(t)\| > \varepsilon$ for infinitely many $t$. This would conflict with the lower bound $\theta(t) = \|\xi(t)\|^2 \geq 0$ for all $t$.] Hence, consensus is reached. A direct calculation using (1) and (3) shows that $\sum_{i=1}^{n} x_i(t+1) = \sum_{i=1}^{n} x_i(t)$ for any $t \geq 0$. This concludes the conservation of the system. Hence, average consensus is achieved asymptotically as $t$ tends to infinity. $\square$

It is worth noting that the condition that all $g_k^I, g_k^{II} \in \mathcal{F}_1$ in Theorem 1 can be weakened. We may only require that this holds for one $k \in \mathcal{V}$ and the modulating functions for all other $k$ are simply non-increasing (and can be in $\mathcal{F}_2$ for example). The same proof can be applied as this would not affect the underlying connectivity of the system.

## 3.2 Heaviside-like modulating functions

In this section, we examine the scenario that all modulating functions belong to $\mathcal{F}_2$ and they may affect the overall connectivity underlying the system (1). In particular, we confine ourselves to the case that both $g_k^I$ and $g_k^{II}$ are Heaviside functions. Namely, for every $k \in \mathcal{V}$ we assume $g_k^I \in \mathcal{F}_2(\sigma_k^I, \phi_k^I)$ and $g_k^{II} \in \mathcal{F}_2(\sigma_k^{II}, \phi_k^{II})$ satisfying $g_k^I(y) \equiv \phi_k^I$ for $y < \sigma_k^I$ and $g_k^{II}(y) \equiv \phi_k^{II}$ for $y < \sigma_k^{II}$. We introduce a function $\gamma(y) : [0, \infty) \to [0, \infty)$:

$$\gamma(y) = \sum_{l=1}^{\lfloor \frac{y}{s} \rfloor} g(ls)s1_{\{y \geq s\}} + g\left(\left(\left\lfloor \frac{y}{s} \right\rfloor + 1\right)s\right) \cdot \left(y - \left\lfloor \frac{y}{s} \right\rfloor s\right), \qquad (17)$$

where $s$ is a parameter of the function and $1_{\{\dots\}}$ represents an indicator function. It is easy to see that $\gamma(y)$ is an increasing function for any given $s > 0$, and it is essentially a Riemann sum satisfying $\lim_{s \to 0} \gamma(y) = \int_0^y g(z)dz$.

To analyze the consensus and conservation, we need the concept of energy $\Gamma$ of the system at time $t$ defined by

$$\Gamma(t) = \frac{1}{2} \sum_{i,j=1}^{n} \sum_{k \in \mathcal{T}_{ij}} (\phi_k^I)^2 \phi_k^{II} \gamma(\|x_i(t) - x_j(t)\|^2) \geq 0. \qquad (18)$$

The function $\gamma(y)$ plays a key role in the energy (18) and the following estimate will be used in the proof of Theorem 2 below.

$$\gamma(\|x_i(t+1) - x_j(t+1)\|^2) - \gamma(\|x_i(t) - x_j(t)\|^2)$$
$$\leq g(\|x_i(t) - x_j(t)\|^2) \cdot \left(\|x_i(t+1) - x_j(t+1)\|^2 - \|x_i(t) - x_j(t)\|^2\right). \qquad (19)$$

This can be seen by examining two cases: (a) $\|x_i(t) - x_j(t)\|^2 < \|x_i(t+1) - x_j(t+1)\|^2$ and (b) $\|x_i(t) - x_j(t)\|^2 \geq \|x_i(t+1) - x_j(t+1)\|^2$. In each case, we then consider three subcases in view of the definition (17): (a1) $\|x_i(t) - x_j(t)\|^2 < \|x_i(t+1) - x_j(t+1)\|^2 < s$; (a2) $\|x_i(t) - x_j(t)\|^2 < s \leq \|x_i(t+1) - x_j(t+1)\|^2$; and (a3) $s \leq \|x_i(t) - x_j(t)\|^2 < \|x_i(t+1) - x_j(t+1)\|^2$ and similarly for case (b). Below we just show (a), and the other situations for (b) can be proved along the same line.

(a1): For $y < s$, $\gamma(y) = g(s)y$. Noting that $g$ is non-increasing, we have

$$\gamma(\|x_i(t+1) - x_j(t+1)\|^2) - \gamma(\|x_i(t) - x_j(t)\|^2)$$
$$= g(s) \cdot \left(\|x_i(t+1) - x_j(t+1)\|^2 - \|x_i(t) - x_j(t)\|^2\right)$$
$$\leq g(\|x_i(t) - x_j(t)\|^2) \cdot \left(\|x_i(t+1) - x_j(t+1)\|^2 - \|x_i(t) - x_j(t)\|^2\right). \qquad (20)$$

(a2):

$$\gamma(\|x_i(t+1) - x_j(t+1)\|^2) - \gamma(\|x_i(t) - x_j(t)\|^2)$$

$$=g(s)(s - \|x_i(t) - x_j(t)\|^2) + \sum_{l=2}^{\lfloor \frac{y}{s} \rfloor} g(ls)s + g\left(\left(\left\lfloor \frac{y}{s} \right\rfloor + 1\right)s\right)$$

$$\cdot \left(\|x_i(t+1) - x_j(t+1)\|^2 - \left\lfloor \frac{\|x_i(t+1) - x_j(t+1)\|^2}{s} \right\rfloor s\right)$$

$$\leq g(\|x_i(t) - x_j(t)\|^2) \cdot \left(\|x_i(t+1) - x_j(t+1)\|^2 - \|x_i(t) - x_j(t)\|^2\right), \quad (21)$$

where $y = \|x_i(t+1) - x_j(t+1)\|^2$ and we have used the monotonicity of $g$.

(a3): Similarly, we have

$$\gamma(\|x_i(t+1) - x_j(t+1)\|^2) - \gamma(\|x_i(t) - x_j(t)\|^2)$$

$$=g\left(\left(\left\lfloor \frac{y_1}{s} \right\rfloor + 1\right)s\right) \cdot \left(\left(\left\lfloor \frac{y_1}{s} \right\rfloor + 1\right)s - y_1\right) + g\left(\left(\left\lfloor \frac{y_1}{s} \right\rfloor + 2\right)s\right)s + \cdots$$

$$+ g\left(\left\lfloor \frac{y_2}{s} \right\rfloor s\right)s + g\left(\left(\left\lfloor \frac{y_2}{s} \right\rfloor + 1\right)s\right)\left(y_2 - \left\lfloor \frac{y_2}{s} \right\rfloor s\right)$$

$$\leq g(\|x_i(t) - x_j(t)\|^2) \cdot \left(\|x_i(t+1) - x_j(t+1)\|^2 - \|x_i(t) - x_j(t)\|^2\right), \quad (22)$$

where $y_1 = \|x_i(t) - x_j(t)\|^2$ and $y_2 = \|x_i(t+1) - x_j(t+1)\|^2$.

As we here consider Heaviside-like modulating functions which significantly affect the connectivity, we will assume the hypergraph $\mathcal{G}$ is fully connected, namely $a_{ijk} = 1$ for all distinct triples. Under this assumption, when the initial energy is sufficiently small, we can expect the connectivity of the system may be maintained. The main result in this section is the following.

**Theorem 2.** *Let $\mathcal{G}$ be fully connected. For every $k \in \mathcal{V}$, assume $g \in \mathcal{F}_2(\sigma, \phi)$, $g_k^I \in \mathcal{F}_2(\sigma_k^I, \phi_k^I)$ and $g_k^{II} \in \mathcal{F}_2(\sigma_k^{II}, \phi_k^{II})$ satisfying $g_k^I(y) \equiv \phi_k^I$ for $y < \sigma_k^I$ and $g_k^{II}(y) \equiv \phi_k^{II}$ for $y < \sigma_k^{II}$. Suppose $h \in \left(0, ((n-1)g(0) \max_{k \in \mathcal{V}}\{(\phi_k^I)^2 \phi_k^{II}\})^{-1}\right)$ and there exists $s \in (0, \hat{\sigma})$ satisfying*

$$\Gamma(0) < (n-1)\gamma(\hat{\sigma}^2) \min_{i,j \in \mathcal{V}} \sum_{k \in \mathcal{V} \setminus \{i,j\}} (\phi_k^I)^2 \phi_k^{II}, \quad (23)$$

*where $\hat{\sigma} = \min_{k \in \mathcal{V}}\{\sigma, \sigma_k^I, \sigma_k^{II}\}$. Then the discrete-time system (1) with (3) achieves consensus and conservation.*

**Proof.** It follows from (1), (3), (18) and (19) that

$$
\begin{aligned}
\Gamma(t+1) - \Gamma(t) \leq & \frac{1}{2} \sum_{i,j=1}^{n} \sum_{k \in \mathcal{T}_{ij}} (\phi_k^I)^2 \phi_k^{II} g(\|x_i(t) - x_j(t)\|^2) \\
& \cdot \left( \|x_i(t+1) - x_j(t+1)\|^2 - \|x_i(t) - x_j(t)\|^2 \right) \\
= & \frac{1}{2} \sum_{i,j=1}^{n} \sum_{k \in \mathcal{T}_{ij}} (\phi_k^I)^2 \phi_k^{II} g(\|x_i(t) - x_j(t)\|^2) \\
& \cdot \left( \|x_i(t) - x_j(t) + h u_i(t) - h u_j(t)\|^2 - \|x_i(t) - x_j(t)\|^2 \right) \\
= & \frac{h^2}{2} \sum_{i,j=1}^{n} \sum_{k \in \mathcal{T}_{ij}} (\phi_k^I)^2 \phi_k^{II} g(\|x_i(t) - x_j(t)\|^2) \\
& \cdot (u_i(t) - u_j(t))^{\mathsf{T}} (u_i(t) - u_j(t)) \\
& + h \sum_{i,j=1}^{n} \sum_{k \in \mathcal{T}_{ij}} (\phi_k^I)^2 \phi_k^{II} g(\|x_i(t) - x_j(t)\|^2) \\
& \cdot (x_i(t) - x_j(t))^{\mathsf{T}} (u_i(t) - u_j(t)) \\
= & h^2 u(t)^{\mathsf{T}} \mathcal{L} u(t) + 2 h x(t)^{\mathsf{T}} \mathcal{L} u(t) \\
= & - x(t)^{\mathsf{T}} \Lambda(t) x(t), \tag{24}
\end{aligned}
$$

where $\Lambda(t) = 2h\mathcal{L}^2 - h^2\mathcal{L}^3$. By the Gershgorin circle theorem, $\lambda_i(\mathcal{L}) \leq 4(n-1)\Delta_{\max} g(0) \max_{k \in \mathcal{V}}\{(\phi_k^I)^2 \phi_k^{II}\}$. Since $h \in \left(0, (2(n-1)\Delta_{\max} g(0) \max_{k \in \mathcal{V}}\{(\phi_k^I)^2 \phi_k^{II}\})^{-1}\right)$, we know $2 - h\lambda_i(\mathcal{L}) > 0$ for all $i \in \mathcal{V}$. Hence, all eigenvalues of $\Lambda(t)$ are non-negative and $\Gamma(t+1) - \Gamma(t) \leq 0$ by (24). This means the energy of the system is non-increasing.

Combining this observation with (23), we have $\Gamma(t) < (n-1)\gamma(\hat{\sigma}^2)$ for any $t \geq 0$. Denote by $\tilde{\mathcal{G}}(t)$ the graph having the adjacency matrix $(b_{ij}(t)) \in \mathbb{R}^{n \times n}$, where $b_{ij}$ is given by (6). We claim $\tilde{\mathcal{G}}(t)$ is connected. If this is not true, then the node set $\mathcal{V}$ can be divided into two parts with size $k$ and $n - k$ for $1 \leq k \leq n - 1$ without edges running between them. Note that $f(k) = k(n-k)$ is a concave parabolic function with the minimum attained at $k = 1$ or $k = n - 1$. This means there are no less than $n - 1$ pairs of nodes that are not connected in $\tilde{\mathcal{G}}(t)$. Since $\mathcal{G}$ is fully connected and

13

$\gamma$ is increasing, we obtain

$$\begin{aligned}
\Gamma(t) \geq & \frac{1}{2} \sum_{i,j\in\mathcal{V}:\|x_i(t)-x_j(t)\|\geq\hat\sigma} \Big( \sum_{k\in\mathcal{T}_{ij}} (\phi_k^I)^2\phi_k^{II} \Big) \gamma(\|x_i(t)-x_j(t)\|^2) \\
\geq & (n-1)\gamma(\hat\sigma^2) \min_{i,j\in\mathcal{V}} \sum_{k\in\mathcal{V}\setminus\{i,j\}} (\phi_k^I)^2\phi_k^{II},
\end{aligned} \tag{25}$$

which conflicts (23). Hence, we have proved the claim.

Given $t \geq 0$, let $\eta = (\eta_1, \eta_2, \cdots, \eta_n)^{\mathsf{T}} \in \mathbb{R}^n$ be the normalized unit eigenvector associated with $\lambda_2(\mathcal{L})$. In view of (6), full connectedness of $\mathcal{G}$, and our assumption on the modulating functions, we obtain

$$\begin{aligned}
\lambda_2(\mathcal{L}) &= \eta^{\mathsf{T}}\mathcal{L}\eta \\
&= \frac{1}{2} \sum_{i,j,k=1}^{n} a_{ijk} g(\|x_i-x_j\|) g_k^I(\|x_i-x_k\|) g_k^I(\|x_j-x_k\|) \\
&\quad \cdot g_k^{II}\Big(\Big\|\frac{x_i+x_j}{2}-x_k\Big\|\Big)(\eta_i-\eta_j)^2 \\
&\geq \frac{1}{2}\phi_k(\phi_k^I)^2\phi_k^{II} \sum_{\{i,j\}\in\tilde{\mathcal{G}}(t)} (\eta_i-\eta_j)^2 \\
&= \phi_k(\phi_k^I)^2\phi_k^{II}\eta^{\mathsf{T}}\tilde{\mathcal{L}}\eta \\
&\geq \phi_k(\phi_k^I)^2\phi_k^{II}\eta^{\mathsf{T}}\lambda_2(\tilde{\mathcal{L}}) := c_3(t) > 0,
\end{aligned} \tag{26}$$

where $\tilde{\mathcal{L}}$ is the Laplacian corresponding to the graph $\tilde{\mathcal{G}}(t)$ with a $(0,1)$-adjacency matrix, and we have used the Rayleigh-Ritz theorem and the connectedness of $\tilde{\mathcal{G}}(t)$. Since $\tilde{\mathcal{L}}$ can only be chosen from a finite set, we conclude $c_3(t) \geq c_3 > 0$ for some constant $c_3$.

Define $\theta(t) = \xi(t)^{\mathsf{T}}\xi(t)$ as in the proof of Theorem 1, and we obtain by (10) that $\theta(t+1) - \theta(t) = -\xi(t)^{\mathsf{T}}(\Theta(t)\otimes I_m)\xi(t)$, where $\Theta(t) = 2h\mathcal{L}-h^2\mathcal{L}^2$. Employing the full connectedness of $\mathcal{G}$ and the Gershgorin circle theorem,

$$\lambda_i(\mathcal{L}) \leq 2\max_{i\in\mathcal{V}} \sum_{j=1}^{n} b_{ij}(t) \leq 2(n-1)g(0)\max_{k\in\mathcal{V}}\{(\phi_k^I)^2\phi_k^{II}\} \tag{27}$$

for all $i \in \mathcal{V}$. Accordingly, we have $\lambda_1(\Theta(t)) = 0$ and for $i \geq 2$ we derive

$$\begin{aligned}
\lambda_i(\Theta(t)) &= h\lambda_i(\mathcal{L})(2-h\lambda_i(\mathcal{L})) \\
&\geq hc_3\big(2 - 2h(n-1)g(0)\max_{k\in\mathcal{V}}\{(\phi_k^I)^2\phi_k^{II}\}\big) := c_4 > 0
\end{aligned} \tag{28}$$

14

by using (26), (27) and the assumption of $h$.

As in the proof of Theorem 1, by using the Rayleigh-Ritz theorem and the projection $P_{\mathcal{N}(\Theta(t)\otimes I_m)}$, we obtain

$$
\begin{aligned}
\theta(t+1) - \theta(t) \leq & - \lambda_2(\Theta(t)) \cdot \big(\xi(t) - P_{\mathcal{N}(\Theta(t)\otimes I_m)}\xi(t)\big)^{\mathsf{T}} \\
& \cdot \big(\xi(t) - P_{\mathcal{N}(\Theta(t)\otimes I_m)}\xi(t)\big) \\
= & - \lambda_2(\Theta(t)) \cdot \xi(t)^{\mathsf{T}}\xi(t) \\
\leq & - c_4 \xi(t)^{\mathsf{T}}\xi(t),
\end{aligned} \tag{29}
$$

where we have applied (28). As in Theorem 1, this means $\xi(t) \to 0_{nm}$ as $t \to \infty$. Therefore, consensus is reached. A direct calculation using (1) and (3) shows that $\sum_{i=1}^{n} x_i(t+1) = \sum_{i=1}^{n} x_i(t)$ for any $t \geq 0$. This shows the conservation of the system and completes the proof. $\square$

If $\phi_k^I \equiv \phi^I$ and $\phi_k^{II} \equiv \phi^{II}$ for all $k \in \mathcal{V}$, then the initial energy condition (23) can be reduced to

$$
\Gamma(0) < (n-1)(n-2)\gamma(\hat{\sigma}^2)(\phi^I)^2\phi^{II}. \tag{30}
$$

By (18) and the full connectedness of $\mathcal{G}$, we have

$$
\Gamma(0) = \frac{n-2}{2}(\phi^I)^2\phi^{II} \sum_{i,j=1}^{n} \gamma(\|x_i(0) - x_j(0)\|^2). \tag{31}
$$

Since $\gamma$ is increasing with $\gamma(0) = 0$, it is easy to see that when the discrepancies between nodes are small enough the condition (30) holds. Moreover, the condition is easier to meet for a smaller number of nodes.

The assumption $g \in \mathcal{F}_2(\sigma, \phi)$ in Theorem 2 models the homophily principle in social networks [44, 45], where people are more willing to make a contact and negotiate with those who have similar views or traits. If the distance between nodes $i$ and $j$ is over the threshold $\sqrt{\sigma}$, the interaction between them ceases. It follows from the energy inequality (23) that a larger $\sigma$ implies a more relaxed condition and hence agents in the system are more open-minded and inclined to reach consensus and conservation. This agrees with our intuition. An analogous result can be seen below in Theorem 4 for continuous-time dynamics. Similar homophily mechanisms have been widely studied in opinion dynamics with bounded confidence; see e.g. [2, 57].

# 4 Consensus and conservation of continuous-time dynamics

We move on to consider the continuous-time system (2) with the same input $u_i$ given by (3). In the analysis of continuous-time dynamical behavior, we will assume local Lipschitz continuity [56] of the modulating functions.

## 4.1 Gravity-like modulating functions

The scenario for gravity-like modulating functions can be dealt with in analogy with the discrete-time counterpart in Section 3.1 with some algebraic tweaks.

**Theorem 3.** *Assume $g, g_k^I, g_k^{II} \in \mathcal{F}_1$ and they are locally Lipschitz continuous for all $k \in \mathcal{V}$. If $\mathcal{G}$ is connected, then the continuous-time system (2) with (3) achieves consensus and conservation.*

**Proof.** Recall that the state of the system is encoded in $x(t) = (x_1(t), x_2(t), \cdots, x_n(t)) \in \mathbb{R}^{nm}$ and the difference between its projection to the synchronization manifold is given by $\xi(t) = x(t) - P_{\mathcal{M}}x(t)$ for $t \geq 0$. We define the Lyapunov function $\theta(t) = \frac{1}{2}\xi(t)^\mathsf{T}\xi(t)$. The Dini derivative of it along the trajectory leads to

$$
\begin{aligned}
\frac{d\theta(t)}{dt} =& \xi(t)^\mathsf{T}\frac{d\xi(t)}{dt} \\
=& \Big(x(t) - 1_n \otimes \frac{1}{n}\sum_{i=1}^n x_i(t)\Big)^\mathsf{T} \\
& \cdot \Big(-(\mathcal{L} \otimes I_m)x(t) + (\mathcal{L} \otimes I_m)\big(1_n \otimes \frac{1}{n}\sum_{i=1}^n x_i(t)\big)\Big) \\
=& -x(t)^\mathsf{T}(\mathcal{L} \otimes I_m)x(t),
\end{aligned}
\tag{32}
$$

where we have made use of the expression $P_{\mathcal{M}}x = 1_n \otimes \frac{1}{n}\sum_{i=1}^n x_i$. Thanks to the connectedness of $\mathcal{G}$, the assumption on the modulating functions and (3), we know that $\mathcal{L} \otimes I_m$ is positive semidefinite. It follows from (32) that $\theta(t)$ is non-increasing and hence $\|\xi(t)\|$ is decreasing for $t \geq 0$.

By an application of the Rayleigh-Ritz theorem following the similar argument as in Theorem 1, we have

$$
\begin{aligned}
\frac{d\theta(t)}{dt} \leq& -\lambda_2(\mathcal{L}) \cdot \big(\xi(t) - P_{\mathcal{N}(\mathcal{L}\otimes I_m)}\xi(t)\big)^\mathsf{T}\big(\xi(t) - P_{\mathcal{N}(\mathcal{L}\otimes I_m)}\xi(t)\big) \\
=& -\lambda_2(\mathcal{L}) \cdot \xi(t)^\mathsf{T}\xi(t)
\end{aligned}
\tag{33}
$$

noting that $\mathcal{N}(\mathcal{L} \otimes I_m) = \mathcal{M} = \text{span}\{1_n \otimes z | z \in \mathbb{R}^m\}$. By (15) we have $\lambda_2(\mathcal{L}) \geq c_1 > 0$ for some constant $c_1$. Feeding this into (33) yields $\frac{d\theta(t)}{dt} \leq -c_1\xi(t)^\mathsf{T}\xi(t)$ for $t \geq 0$. An argument of contraction gives rise to the vanishing of $\xi$, namely, $\xi(t) \to 0_{nm}$ as $t \to \infty$. Consensus is reached as expected. A direct calculation using (2) and (3) shows that $\frac{d}{dt}\sum_{i=1}^n x_i(t) = 0$ for any $t \geq 0$. This completes the conservation part of the theorem. As in the discrete-time case, average consensus can be achieved. $\square$

As commented in the discrete case below Theorem 1, the condition that $g_k^I, g_k^{II} \in \mathcal{F}_1$ just needs to be held here for one node $k \in \mathcal{V}$.

## 4.2 Heaviside-like modulating functions

Analogously as in the discrete-time system studied in Section 3.2, we here redefine the following energy function $\Gamma$ of the continuous-time system (2) at time $t$:

$$\Gamma(t) = \frac{1}{2}\sum_{i,j=1}^n \sum_{k \in \mathcal{T}_{ij}} (\phi_k^I)^2 \phi_k^{II} \int_0^{\|x_i(t)-x_j(t)\|^2} g(z)dz \geq 0. \tag{34}$$

The overall energy of the system at time $t$ is captured by (34). We show that consensus and conservation can be achieved if the initial energy is small.

**Theorem 4.** *Let $\mathcal{G}$ be fully connected. For every $k \in \mathcal{V}$, assume $g \in \mathcal{F}_2(\sigma, \phi)$, $g_k^I \in \mathcal{F}_2(\sigma_k^I, \phi_k^I)$ and $g_k^{II} \in \mathcal{F}_2(\sigma_k^{II}, \phi_k^{II})$ satisfying $g_k^I(y) \equiv \phi_k^I$ for $y < \sigma_k^I$ and $g_k^{II}(y) \equiv \phi_k^{II}$ for $y < \sigma_k^{II}$. Suppose*

$$\Gamma(0) < (n-1)\Big(\int_0^{\hat{\sigma}^2} g(z)dz\Big) \min_{i,j \in \mathcal{V}} \sum_{k \in \mathcal{V}\backslash\{i,j\}} (\phi_k^I)^2 \phi_k^{II}, \tag{35}$$

*where $\hat{\sigma} = \min_{k \in \mathcal{V}}\{\sigma, \sigma_k^I, \sigma_k^{II}\}$. Then the continuous-time system (2) with (3) achieves consensus and conservation.*

**Proof.** Let $x = (x_1, x_2, \cdots, x_n) \in \mathbb{R}^{nm}$ be the solution of the system. Consider the locally Lipschitz potential function $\theta(x) = \frac{1}{2}x^\mathsf{T}x$. Using (2) and (7), the time derivative of $\theta$ is

$$\frac{d\theta(x)}{dt} = -x^\mathsf{T}(\mathcal{L} \otimes I_m)x \leq 0. \tag{36}$$

By LaSalle's invariance principle [56, Thm 3.2], the set of accumulation points of $x$ is always contained in the set $\mathcal{N}(\mathcal{L} \otimes I_m)$.

The derivative of the energy function (34) is

$$\frac{d\Gamma(t)}{dt} = \sum_{i,j=1}^{n} \sum_{k \in \mathcal{T}_{ij}} (\phi_k^I)^2 \phi_k^{II} g(\|x_i(t) - x_j(t)\|^2)(x_i(t) - x_j(t))^\mathsf{T}(u_i(t) - u_j(t))$$

$$= 2x(t)^\mathsf{T}\mathcal{L}u(t) = -2u(t)^\mathsf{T}u(t) \le 0. \tag{37}$$

Therefore, employing (35) we obtain

$$\Gamma(t) \le \Gamma(0) < (n-1)\left(\int_0^{\hat{\sigma}^2} g(z)dz\right) \min_{i,j \in \mathcal{V}} \sum_{k \in \mathcal{V}\setminus\{i,j\}} (\phi_k^I)^2 \phi_k^{II}, \tag{38}$$

This means there are less than $n-1$ pairs of nodes in $\mathcal{V}$ satisfying $\|x_i(t) - x_j(t)\| \ge \hat{\sigma}$. Denote by $\tilde{\mathcal{G}}(t)$ the graph having the adjacency matrix $(b_{ij}(t)) \in \mathbb{R}^{n \times n}$, where $b_{ij}$ is given by (6). Since $\mathcal{G}$ is fully connected, by considering the concave parabolic function $f(k) = k(n-k)$ $(1 \le k \le n-1)$ as in Theorem 2, we derive that $\tilde{\mathcal{G}}(t)$ is connected. As a result, $\mathcal{N}(\mathcal{L} \otimes I_m) = \mathcal{M} = \mathrm{span}\{1_n \otimes z | z \in \mathbb{R}^m\}$. This proves consensus. Conservation follows again from $\frac{d}{dt}\sum_{i=1}^{n} x_i(t) = 0$ for $t \ge 0$. $\square$

If $\phi_k^I \equiv \phi^I$ and $\phi_k^{II} \equiv \phi^{II}$ for all $k \in \mathcal{V}$, then the initial energy condition (35) becomes

$$\Gamma(0) < (n-1)(n-2)(\phi^I)^2 \phi^{II} \int_0^{\hat{\sigma}^2} g(z)dz. \tag{39}$$

By (34) and the full connectedness of $\mathcal{G}$, we obtain

$$\Gamma(0) = \frac{n-2}{2}(\phi^I)^2 \phi^{II} \sum_{i,j=1}^{n} \int_0^{\|x_i(0)-x_j(0)\|^2} g(z)dz. \tag{40}$$

When the discrepancies between nodes are small enough the condition (39) holds. The condition is easier to meet for a smaller number of nodes.

It can be seen from the above results that the group reinforcement effect caused by the modulating functions $g, g_k^I, g_k^{II}$ places a challenge in the theoretical analysis for consensus and conservation, where we resort to detailed eigenvalue analysis and synchronization manifold projection in the case of gravity-like modulation, and construction of Lyapunov and energy functions in the case of Heaviside-like modulation. Peer pressure and group reinforcement have often been observed in social psychology and biology [58, 59]. For example, in social networks the influence of an opinion on another depends nonlinearly on its popularity. The coordination of an individual's motion

within a group, be it a swarm of insects, a school of fish, or a flock of birds, depends on the nonlinear actions among its close neighbors. Moreover, the idea of group reinforcement also underpins the multiagent reinforcement learning [60], where agents learn the behavior and keep cohesion by exposure to a group of neighbors with nonlinear rewards and modulation.

# 5 Numerical simulations

Following is a series of numerical examples that demonstrate the developed theoretical framework above.

**Example 1.** In this example, we illustrate the action of gravity-like modulating functions on the three-body interactions based on Theorem 1 and Theorem 3. Consider a fully connected hypergraph $\mathcal{G}$ composed by $n = 5$ nodes, namely, $\mathcal{V} = \{1, 2, 3, 4, 5\}$. Let $m = 2$ and write $x_i = (x_{i1}, x_{i2}) \in \mathbb{R}^2$ for the state of agent $i \in \mathcal{V}$. The modulating functions $g, g_k^I, g_k^{II} \in \mathcal{F}_1$ are chosen as $g(y) = e^{-y}$, $g_k^I(y) = g_k^{II}(y) = (y + 10)^{-1}$ for all $k \in \mathcal{V}$. Noting $\Delta_{\max} = 6$, we take $h = 80$ for the discrete-time dynamical system (1). The initial configuration is given by $x(0) = (-4, 3, 1, 2.5, 5, -0.5, 1.5, -3, -3.5, -2)^\mathsf{T}$, for which the average state over the system is at the origin $(0, 0)$.

We show in Fig. 2 the evolution of the discrete-time system (1) and the continuous-time system (2) with (3). Since the conditions in Theorem 1 and Theorem 3 are satisfied, the average consensus at $(0, 0)$ agrees with our theoretical predictions. Even if both the hypergraph topology ($\mathcal{G}$) and the modulating functions ($g_k^I \equiv g_k^{II}$) are symmetric, the component dynamics show interesting phased convergence due to the introduction of asymmetric roles and initial configuration. In the first component, for example, agents 2, 3, and 4 first reach a consensus and then join with agents 1 and 5.

For the discrete-time case, usually a larger $h$ can speed up the convergence but cannot exceed the limitation pertinent to bandwidth in information theory [34, 61]. In Fig. 3 we show the same discrete-time dynamics but for $h = 170$. The condition of $h$ in Theorem 1 is violated and we observe that consensus is not reached. In fact, there is a low level interpretation and a high level interpretation. The low level explantation is that the regulation constant $h$ here plays the role of gain in control systems, which affects the system matrix (and its eigenvalues) of the discrete-time dynamics. A larger $h$ will reduce system stability as can be seen from the theorem proof. The high level explantation is that in information theory, a channel's bandwidth affects its capacity. The information flow in a signaling network (the hypergraph $\mathcal{G}$ in our case) often breaks down due to low bandwidth or data
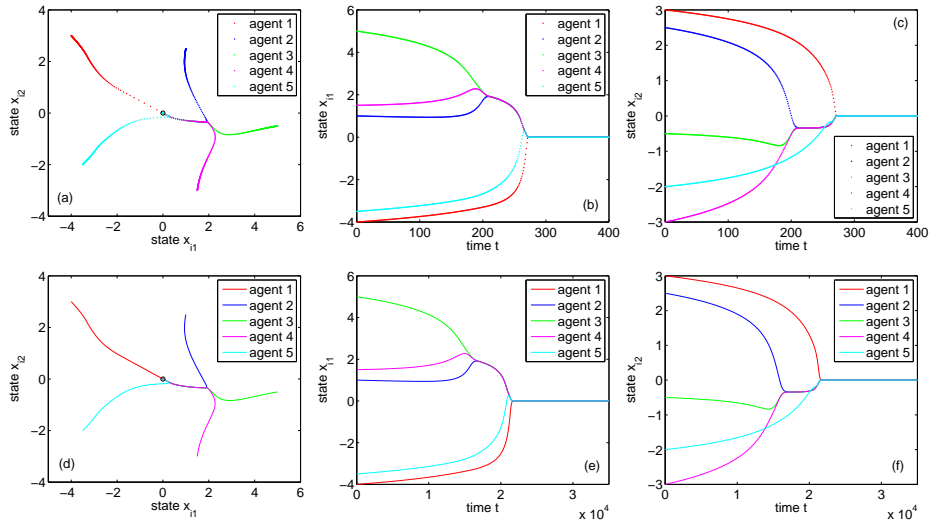
Figure 2: State evolution of agents in Example 1 with gravity-like modulating functions for: (a, b, c) the discrete-time system (1) and (d, e, f) the continuous-time system (2). (a) and (d) show the states in $\mathbb{R}^2$ with the origin indicated by a circle; (b) and (c) are for the time evolution of the discrete-time system with $h = 80$; (e) and (f) are for the continuous-time system.

rate by the Nyquist theorem, which amounts to a large $h$ under the Laplace transform.

**Example 2.** We now consider the action of Heaviside-like modulating functions on the three-body interactions based on Theorem 2 and Theorem 4. The same hypergraph $\mathcal{G}$ and the two-dimensional dynamics as in Example 1 are adopted here. The modulating functions are chosen as $g(y) = 1_{\{y<2\}} \in \mathcal{F}_2(\sigma = 2, \phi = 1)$, $g_k^I = g_k^{II} = 1_{\{y<2\}} \in \mathcal{F}_2(\sigma_k^I = \sigma_k^{II} = 2, \phi_k^I = \phi_k^{II} = 1)$ for all $k \in \mathcal{V}$. In other words, all modulating functions are the same switching function at value 2. By taking the initial configuration $x(0) = (-0.28, 0.36, 0.1, 0.27, 0.54, -0.09, 0.18, -0.36, -0.54, -0.18)^{\mathsf{T}}$, it is direct to verify that the equilibrium is at the origin and the initial energy $\Gamma(0) \approx 15.5 < 24$ in (23) and (35). We choose $h = 0.1$ for the discrete-time dynamical system (1). All conditions in Theorem 2 and Theorem 4 are met.

Fig. 4 shows the state trajectories of both systems. We observe that average consensus has been achieved as one would expect. Compared with Fig. 2 in Example 1, the states converge much faster because the modulating
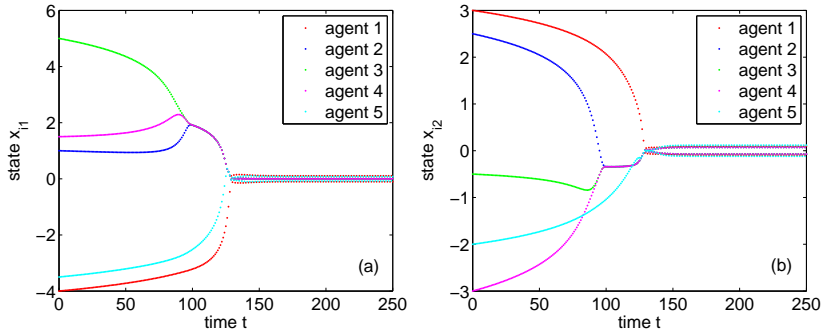
Figure 3: State evolution of agents in Example 1 with gravity-like modulating functions for the discrete-time system (1) with $h = 170$. Consensus fails for both components (a) $x_{i1}$ and (b) $x_{i2}$.

functions used here apply a much stronger coupling on the network structure. From Fig. 4(a) and (d) we note that the trajectories only move in lower-dimensional planes (in lines in this case). This can be seen from the system equations (1), (2) and (3) as the coupling in this example is fixed when the modulating functions are switched on (which is always the case given the initial configuration).

In Fig. 5 we consider a different initial condition $x(0) = (-0.76, 1, 0.35, 0.76, 1.5, -0.25, 0.5, -1, -1.6, -0.5)^{\mathsf{T}}$. The initial energy now becomes $\Gamma(0) \approx 56.5 > 24$ violating the conditions (23) and (35). It can be seen that the distance between agent 5 and any other agent in $\mathcal{V}$ is always greater than $\sqrt{2}$. By (17), (18) and our choice of the modulating functions, the dynamics of agent 5 is isolated from the other agents, leading to a divergent system.

**Example 3.** Finally, in this example we explore the influence of network structure over the convergence time. We take the fully connected hypergraph $\mathcal{G}$ with $n = 5$ as a starting point. Its network representation is shown in Fig. 6(a), i.e. a complete graph $K_5$. In each step, a specific edge is removed following the procedure shown in Fig. 6(a) until it becomes a sparsest connected hypergraph (in terms of three-body edge interactions). The convergence or consensus time is defined as $\min_{t \geq 0}\{t : \max_{i,j \in \mathcal{V}} \|x_i(t) - x_j(t)\| < 0.01\}$.

The modulating functions $g, g_k^I, g_k^{II} \in \mathcal{F}_1$ are chosen as $g(y) = e^{-\frac{y^2}{10}}$, $g_k^I(y) = g_k^{II}(y) = (y + 10)^{-1}$ for all $k \in \mathcal{V}$. We fix $h = 30$, which satisfies the condition in Theorem 1 of the discrete-time system (1) for all topologies considered in this example. The initial conditions are taken uniformly at
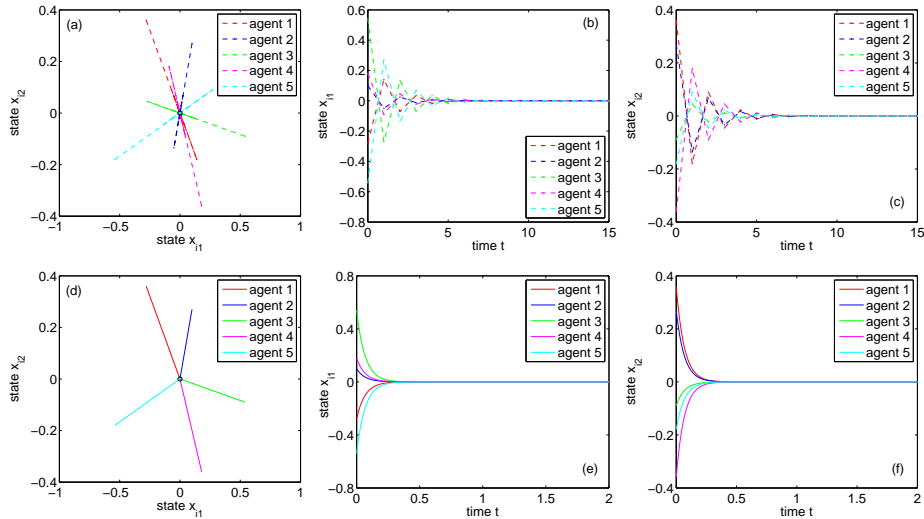
21

Figure 4: State evolution of agents in Example 2 with switching modulating functions for: (a, b, c) the discrete-time system (1) and (d, e, f) the continuous-time system (2). (a) and (d) show the states in $\mathbb{R}^2$ with the origin indicated by a circle; (b) and (c) are for the time evolution of the discrete-time system with $h = 0.1$; (e) and (f) are for the continuous-time system. Dashes lines are shown in (a, b, c) for the aid of eyes.

random within the region $[-1, 1] \times [-1, 1]$ while keeping the average at $(0, 0)$. The results are shown in Fig. 6(b) and (c) for the discrete-time system (1) and the continuous-time system (2), respectively. In the insets of Fig. 6(b) and (c), we display the analogous results for an edge removal process starting from the fully connected hypergraph with $n = 9$. We observe that the consensus time increases as the hypergraph becomes sparser. On average, consensus time shows a roughly linear scale in its growth.

# 6   Conclusion

In this paper we have proposed a three-body consensus model to implement some desirable dynamical characteristics including higher-order interactions, higher-dimensional states, group reinforcement effect and homophily principle. The model features asymmetric roles of interacting agents in a triangle, which is influenced by modulating functions. We have developed analytical frameworks for consensus and conservation of agents with discrete-time
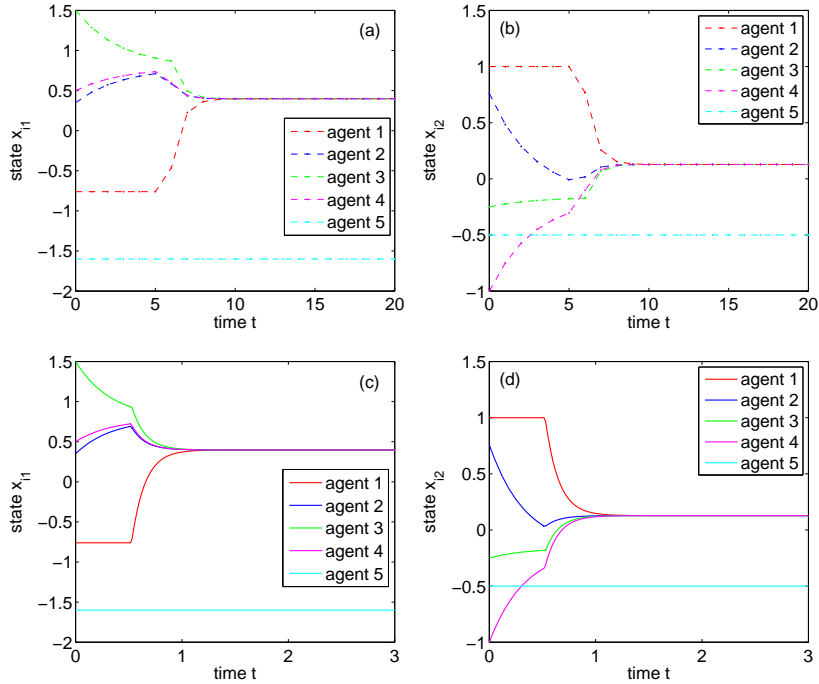
Figure 5: State evolution of agents in Example 2 with switching modulating functions for (a, b) the discrete-time system (1) and (c, d) the continuous-time system (2) with initial configuration $x(0) = (-0.76, 1, 0.35, 0.76, 1.5, -0.25, 0.5, -1, -1.6, -0.5)^\mathsf{T}$. Consensus fails for both components (a) $x_{i1}$ and (b) $x_{i2}$. Dashes lines are shown in (a, b) for the aid of eyes.

dynamics and continuous-time dynamics. In particular, two types of modulating functions, i.e., gravity-like and Heaviside-like functions, have been investigated. Numerical simulations have also confirmed our theoretical findings. This work leads to some interesting directions that could be further explored. First, as consensus processes are usually sensitive to the communication topology, further numerical or even analytical studies can be done to explore the influence of heterogeneous topologies such as hypergraphs with community structures. Second, the current framework only works for three-body interactions. It would be interesting to extend the framework to allow interactions involving a mix of pairs, triples and even general motifs. Another interesting direction is to probe more sophisticated asymmetric roles involving, for example, random noises or game-theoretic strategies.
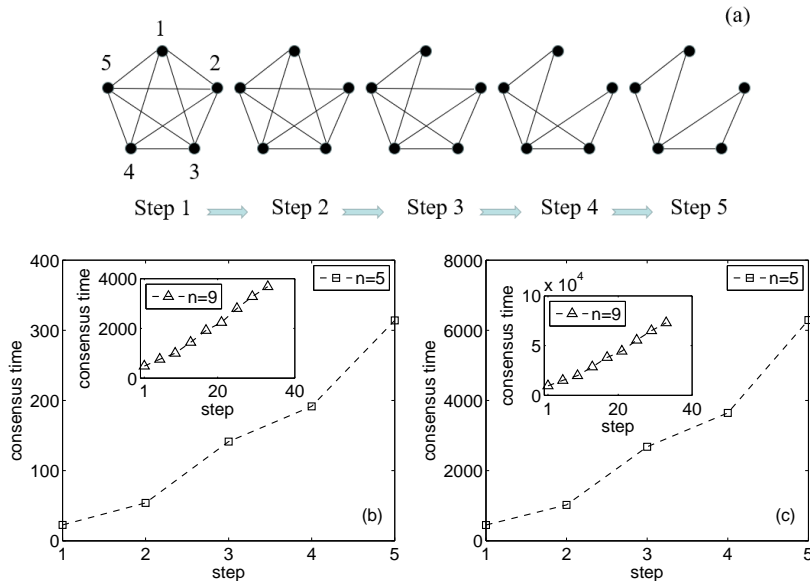
Figure 6: (a) Depreciation process in Example 3 of a fully connected hypergraph by removing one edge at each step. Convergence times for discrete-time system (1) and continuous-time system (2) are shown in (b) and (c) respectively. The insets show the analogous results for depreciating a hypergraph with $n = 9$. Each data point is an average of 50 independent simulation runs for random initial configurations in the region $[-1, 1] \times [-1, 1]$.

## Acknowledgement

The author is very grateful to the reviewers for their detailed and constructive comments which have helped improve the presentation of the paper.

## References

[1] M. Newman, *Networks, 2nd Ed.*, Oxford University Press, Oxford, 2018

[2] S. Boccaletti, V. Latora, Y. Moreno, M. Chavez, D.-U. Hwang, Complex networks: structure and dynamics. *Phys. Rep.*, 424(2006) 175–308

[3] M. W. Reimann, M. Nolte, M. Scolamiero, K. Turner, R. Perin, G. Chindemi, P. Dłotko, R. Levi, K. Hess, H. Markram, Cliques of neu-

24

rons bound into cavities provide a missing link between structure and function. *Front. Comput. Neurosci.*, 11(2017) 48

[4] A. E. Sizemore, C. Giusti, A. Kahn, J. M. Vettel, R. F. Betzel, D. S. Bassett, Cliques and cavities in the human connectome. *J. Comput. Neurosci.*, 44(2018) 115–145

[5] A. Tozzi, The multidimensional brain. *Phys. Life Rev.*, 31(2019) 86–103

[6] J. Grilli, G. Barabás, M. J. Michalska-Smith, S. Allesina, Higher-order interactions stabilize dynamics in competitive network models. *Nature*, 548(2017) 210–213

[7] J. M. Levine, J. Bascompte, P. B. Alder, S. Allesina, Beyond pairwise mechanisms of species coexistence in complex communities. *Nature*, 546(2017) 56–64

[8] A. Patania, G. Petri, F. Vaccarino, The shape of collaborations. *EPJ Data Sci.*, 6(2017) 18

[9] E. Vasilyeva, A. Kozlov, K. Alfano-Bittner, D. Musatov, A. M. Raigorodskii, M. Perc, S. Boccaletti, Multilayer representation of collaboration networks with higher-order interactions. *Sci. Rep.*, 11(2021) 5666

[10] F. Battiston, G. Cencetti, I. Iacopini, V. Latora, M. Lucas, A. Patania, J.-G. Young, G. Petri, Networks beyond pairwise interactions: structure and dynamics. *Phys. Rep.*, 874(2020) 1–92

[11] L. Torres, A. S. Blevins, D. Bassett, T. Eliassi-Rad, The why, how, and when of representations for complex systems. *SIAM Rev.*, 63(2021) 435–485

[12] F. Battiston, E. Amico, A. Barrat, G. Bianconi, G. F. de Arruda, B. Franceschiello, I. Iacopini, S. Kéfi, V. Latora, Y. Moreno, M. M. Murray, T. P. Peixoto, F. Vaccarino, G. Petri, The physics of higher-order interactions in complex systems. *Nat. Phys.*, 17(2021) 1093–1098

[13] C. W. Lynn, D. S. Bassett, The physics of brain network structure, function and control. *Nat. Rev. Phys.*, 1(2019) 318–332

[14] I. Iacopini, G. Petri, A. Barrat, V. Latora, Simplicial models of social contagion. *Nat. Commun.*, 10(2019) 2485

[15] Y. Li, D. Bearup, J. Liao, Habitat loss alters effects of intransitive higher-order competition on biodiversity: a new metapopulation framework. *Proc. R. Soc. B*, 287(2020) 20201571

[16] A. R. Benson, D. F. Gleich, J. Leskovec, Higher-order organization of complex networks. *Science*, 353(6295)(2016) 163–166

[17] C. Bick, E. Gross, H. A. Harrington, M. T. Schaub, What are higher-order networks? *arXiv:2104.11329*

[18] K. Devriendt, P. V. Mieghem, The simplex geometry of graphs. *J. Complex Netw.*, 7(2019) 469–490

[19] P. Bubenki, Statistical topological data analysis using persistence landscapes. *J. Mach. Learn. Res.*, 16(2015) 77–102

[20] D. H. Serrano, J. Hernández-Serrano, D. S. Gómez, Simplicial degree in complex networks. Applications of topological data analysis to network science. *Chaos Soliton. Fract.*, 137(2020) 109839

[21] V. Salnikov, D. Cassese, R. Lambiotte, Simplicial complexes and complex systems. *Euro. J. Phys.*, 40(2019) 014001

[22] G. Ghoshal, V. Zlatić, G. Caldarelli, M. E. J. Newman, Random hypergraphs and their applications. *Phys. Rev. E*, 79(2009) 066118

[23] P. S. Chodrow, Configuration models of random hypergraphs. *J. Complex Netw.*, 8(2020) cnaa018

[24] Y. Shang, Consensus formation in networks with neighbor-dependent synergy and observer effect. *Commun. Nonlinear Sci. Numer. Simulat.*, 95(2021) 105632

[25] J. E. Hopcroft, R. Motwani, J. D. Ulman, *Introduction to Automata Theory, Languages, and Computation, 3rd Ed.*, Pearson, London, 2006

[26] G. F. de Arruda, G. Petri, Y. Moreno, Social contagion models on hypergraphs. *Phys. Rev. Research*, 2(2020) 023032

[27] P. S. Skardal, A. Arenas, Higher order interactions in complex networks of phase oscillators promote abrupt synchronization switching. *Commun. Phys.*, 3(2020) 218

[28] L. V. Gambuzza, F. Di Patti, L. Gallo, S. Lepri, M. Romance, R. Criado, M. Frasca, V. Latora, S. Boccaletti, Stability of synchronization in simplicial complexes. *Nat. Commun.*, 12(2021) 1255

[29] M. T. Schaub, A. R. Benson, P. Horn, G. Lippner, A. Jadbabaie, Random walks on simplicial complexes and the normalized Hodge 1-Laplacian. *SIAM Rev.*, 62(2020) 353–391

[30] T. Carletti, F. Battiston, G. Cencetti, D. Fanelli, Random walks on hypergraphs. *Phys. Rev. E*, 101(2020) 022308

[31] Y. Shang, A note on the majority dynamics in inhomegeneous random graphs. *Results Math.*, 76(2021) 119

[32] J. Noonan, R. Lambiotte, Dynamics of majority rule on hypergraphs. *Phys. Rev. E*, 104(2021) 024316

[33] I. Iacopini, G. Petri, A. Baronchelli, A. Barrat, Group interactions modulate critical mass dynamics in social convention. *arXiv:2103.10411*

[34] R. Olfati-Saber, J. A. Fax, R. M. Murray, Consensus and cooperation in networked multi-agent systems. *Proc. IEEE*, 95(1)(2007) 215–233

[35] V. D. Blondel, J. M. Hendrickx, J. N. Tsitsiklis, Continuous-time average-preserving opinion dynamics with opinion-dependent communications. *SIAM J. Control Optim.*, 48(2010) 5214–5240

[36] J. Török, G. Iñiguez, T. Yasseri, M. S. Miguel, K. Kaski, J. Kertész, Opinion, conflicts, and consensus: modeling social dynamics in a collaborative environment. *Phys. Rev. Lett.*, 110(2013) 088701

[37] G. Jing, Y. Zheng, L. Wang, Consensus of multiagent systems with distance-dependent communication networks. *IEEE Trans. Neural Netw. Learn. Syst.*, 28(2017) 2712–2726

[38] Y. Shang, Resilient consensus in multi-agent systems with state constraints. *Automatica*, 122(2020) 109288

[39] P. Shi, B. Yan, A survey on intelligent control for multiagent systems. *IEEE Trans. Syst. Man Cybern. Syst.*, 51(2021) 161–175

[40] J. Hasanyan, L. Zino, D. A. B. Lombana, A. Rizzo, M. Porfiri, Leader-follower consensus on activity-driven networks. *Proc. R. Soc. A*, 476(2020) 20190485

[41] L. DeVille, Consensus on simplicial complexes: results on stability and synchronization. *Chaos*, 31(2021) 023137

[42] L. Neuhäuser, A. Mellor, R. Lambiotte, Multibody interactions and nonlinear consensus dynamics on networked systems. *Phys. Rev. E*, 101(2020) 032310

[43] R. Sahasrabuddhe, L. Neuhäuser, R. Lambiotte, Modelling non-linear consensus dynamics on hypergraphs. *J. Phys. Complex*, 2(2021) 025006

[44] M. McPherson, L. Smith-Lovin, J. M. Cook, Birds of a feather: homophily in social networks. *Annu. Rev. Sociol.*, 27(2001), 415–444

[45] Y. Halberstam, B. Knight, Homophily, group size, and the diffusion of political information in social networks: evidence from Twitter. *J. Public Econ.*, 143(2016) 73–88

[46] F. Cucker, S. Smale, Emergent behavior in flocks. *IEEE Trans. Autom. Contr.*, 52(2007) 852–862

[47] Y. Shang, Emergence in random noisy environments. *Int. J. Math. Anal.*, 4(2010) 1205–1215

[48] T. Vicsek, A. Czirók, E. Ben-Jacob, I. Cohen, O. Schochet, Novel type of phase transition transition in a system of self-driven particles. *Phys. Rev. Lett.*, 75(1995) 1226–1229

[49] Y. Jia, T. Vicsek, Modelling hierarchical flocking. *New J. Phys.*, 21(2019) 093048

[50] A. Zafeiris, T. Vicsek, *Why We Live in Hierarchies? A Quantitative Treatise*, Springer, Berlin, 2018.

[51] J. Shen, Cucker-Smale flocking under hierarchical leadership. *SIAM J. Appl. Math.*, 68(2008) 694–719

[52] K. Grining, M. Klonowski, M. Sulkowska, Stronger trust and privacy in social networks via local cooperation. *J. Complex Netw.*, 8(2020) cnz032

[53] Y. Li, M. M. Mayfield, B. Wang, J. Xiao, K. Kral, D. Janik, J. Holik, C. Chu, Beyond direct neighbourhood effects: higher-order interactions improve modelling and predicting tree survival and growth. *Natl. Sci. Rev.*, 8(2021) nwaa244

[54] O. T. Courtney, G. Bianconi, Generalized network structures: The configuration model and the canonical ensemble of simplicial complexes. *Phys. Rev. E*, 93(2016) 062311

[55] F. Cucker, J.-G. Dong, Avoiding collisions in flocks. *IEEE Trans. Autom. Contr.*, 55(2010) 1238–1243

[56] N. Rouche, P. Habets, M. Laloy, *Stability Theory by Liapunov's Direct Method*, Springer-Verlag, New York, 1977.

[57] Y. Shang, Deffuant model with general opinion distributions: First impression and critical confidence bound. *Complexity*, 19(2013) 38–49

[58] B. Latané, The psychology of social impact. *Am. Psychol.*, 36(1981) 343–356

[59] M. Durve, F. Peruani, A. Celani, Learning to flock through reinforcement. *Phys. Rev. E*, 102(2020) 012601

[60] S. Gronauer, K. Diepold, Multi-agent deep reinforcement learning: A survey. *Artif. Intell. Rev.*, (2021) *https://doi.org/10.1007/s10462-021-09996-w*

[61] M. Komareji, Y. Shang, R. Bouffanais, Consensus in topologically interacting swarms under communication constraints and time-delays. *Nonlinear Dyn.*, 93(2018) 1287–1300